THE JOURNAL OF PHYSICAL CHEMISTRY C

Article

pubs.acs.org/JPCC

Computational Studies on SAMs of {Mn_6} SMMs on Au(111): Do Properties Change upon Grafting?

Federico Totti,[†,*] Gopalan Rajaraman,[‡] Marcella Iannuzzi,[§] and Roberta Sessoli[†]

[†]Dipartimento di Chimica, Polo Scientifico, INSTM Università degli Studi di Firenze, via della Lastruccia 3, 50019 Sesto Fiorentino, Italy

[‡]Department of Chemistry, Indian Institute of Technology Bombay, Mumbai-400076, India

[§]Institute of Physical Chemistry, University of Zurich, Winterthurerstrasse 190, CH-8057 Zurich, Switzerland

Supporting Information

ABSTRACT: Single molecule magnets (SMM) adsorbed on surfaces as magnetic building blocks represent a hot topic of research in the area of molecular magnetism. Indeed, the understanding the properties of molecules on surface is extremely challenging as atomistic structures are not readily available. In this regard, theoretical studies as reliable tool to reproduce and predict the structure and the magnetic ground state of SMMs in the bulk phase and adsorbed on a surface, should be considered very appealing. In this framework, we report a periodic density functional (DF) study on two {Mn_6} SMM complexes of general formula [$Mn(III)_6O_2$(R-sao)$_6$(O_2C-th)$_2$L], where HO_2C-th=3-thiophene carboxylic acid, $saoH_2$ = salicylaldoxime, *R* = H and L = $(EtOH)_4$ (**1**) or *R* = Et and L = $(EtOH)_4(H2O)_2$ (**2**), performed to ascertain the structure of their self-assembled monolayers (SAM) on the Au(111) surface. Their magnetic properties in vacuum and in the adsorbed state have also been computed and our results clearly demonstrate that the grafting process is expected to not be a smooth one as it alters their bulk structure and, consequently, their magnetic properties.

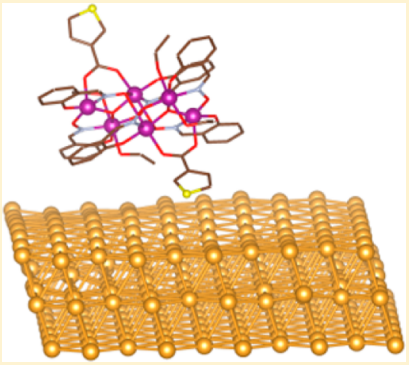

INTRODUCTION

The interest in molecular nano magnets (MNMs)[1] had grown tremendously in recent years due their potential applications in high-density information storage devices, Q-bits in quantum computing and in spintronics devices to name a few.[2] The discovery that a cluster of manganese(III,IV) ions, {Mn_{12}}, retains its magnetization in the absence of magnetic field (single molecule magnet, SMM, behavior) may prove to be of great technological importance, provided that the phenomenon is observed at temperatures significantly higher than liquid helium temperatures. The reversal of magnetization in SMMs is hampered by a barrier reversal whose height is given by $|D|S^2$ for integer spin systems with S being the spin ground state and D a negative axial anisotropy parameter.[3] For the {Mn_{12}} family of complexes, the theoretical barrier height is estimated to be 60 K. Recently many lanthanide complexes reported to have higher barrier height,[4] in particular a {Dy_5(III)} cluster with a barrier of 540 K.[5] Moreover, a monomeric Tb(III) complex with phthalocyaninate ligands is reported to have a barrier height of about 800 K,[6] the largest known for such a class of molecules. However, in most lanthanide-based SMMs, the quantum tunneling of magnetization is very fast, leading to a very small coercitivity in the hysteresis loop, a remarkable exception being the lanthanide dimers bridged by the N_3^- radical[7,8] Regarding clusters of transition metal complexes, a breakthrough has been achieved with the discovery of a family of {Mn_6} complexes [$Mn(III)_6O_2$(sao)$_6$(O_2C-th)$_2$$L_{4-6}$],[9] where HO_2C-ph=3-phenil carboxylic acid, *L* = EtOH, H_2O, possessing a barrier height of ca. 90 K. This is the highest reported for any transition metal SMM so far. Another bottleneck in taking MNMs to end-user applications relays on organizing the molecules on solid-surfaces in order to access individual molecules. Many of these polynuclear clusters are very fragile and undergo some structural transformations upon adsorption. The surface-molecule interaction in many cases lead to the loss of SMM characteristics and this has been witnessed in a variety of cases including the archetypal {Mn_{12}} SMM.[10] Recently, using a long chain alkyl thiol, a {Fe_4} SMM has been organized on Au(111) surface and its SMM features on Au(111) surface have been observed using XMCD studies.[11] Understanding the surface−adsorbate interaction is thus very important to develop a strategy to organize SMMs on surfaces and in this regard theoretical tools are proven to have immense potential as they offer atomistic structure of molecules on surfaces and an insight into their physical as well as magnetic properties.

In this framework, two {Mn_6} complexes (**1** and **2**) have been synthesized and their self-assembled-monolayers (SAM) have been prepared and studied.[12,13] Despite similar structural topology, **1** exhibits a spin ground state of *S* = 4 while **2** has a ground state of *S* = 12 with a barrier height of 86 K (See Figure 1).

Received: January 29, 2013
Published: March 15, 2013

   dx.doi.org/10.1021/jp4009916 | J. Phys. Chem. C 2013, 117, 7186−7190

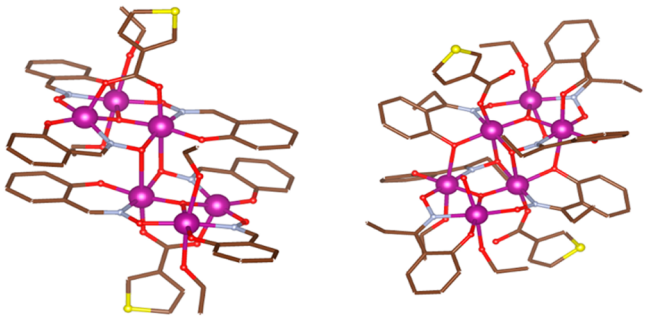

1 2

Figure 1. Crystal structure of complexes **1** and **2**.[14] Manganese atoms are purple colored. Sulfur, oxygen, nitrogen, and carbon are yellow, red, cyan, and brown colored, respectively.

The difference in the ground states arises from the different strength of the magnetic exchange interactions between the individual Mn(III)−Mn(III) pairs. These are an ideal system to investigate at the atomistic level the effect of surface-molecule interaction because the two clusters are structurally similar yet exhibit very different magnetic properties, highlighting the fact that even a small perturbation in the structure can cause a large variation in the magnetic interactions. Theoretical modeling of such clusters on a solid substrate like Au(111) is challenging not only because of the large number of atoms included in the model but also because the computed structure and properties should be of very high quality to ascertain small differences. Thus, this system poses a real challenge to the theoretical method we have established in previous works.[15,16]

COMPUTATIONAL METHODS

In this paper, we used DF-based structural optimization to model complex **1** and **2** in gas phase and grafted on Au (111) surface and to determine ground state and magnetic exchange parameters. The simulation cell for the complex grafted on Au contains 450 atoms, and the molecular orbitals are described with a Gaussian-type orbital basis set of more than 2000 functions. The three layers model to mimic the gold surface has been validated in refs 11, 15, and 16. The convergence criteria of 1×10^{-6} hartree for self-consistent-field energy and 2×10^{-3} hartree bohr^{-1} for the atomic forces, have been considered to get reliably converged structures. To solve the KS equations, we apply the Gaussian and plane waves (GPW) formalism as implemented in the CP2K package.[17] Double-ζ basis sets are used to describe the molecular orbitals, and the augmented PW basis set is truncated to an energy of 400 Ry. Goedecker−Teter−Hutter norm conserved pseudopotentials are employed to describe the interaction between valence electrons and atomic cores. Initially we focused our attention on bare X-ray structure of **1** and **2** to see how optimization of the geometry affects the ground state and the estimated magnetic couplings. We used TPSS,[18] PBE,[19] and B97[20] with van der Waals (VdW) corrections.[21] The optimized structures for the grafted species were obtained by modeling the Au(111) surface by three layers[11,15,16] keeping the lowest one frozen during the optimization.

With regards to the magnetic properties, it is quite well established in the literature that the best agreement with the experimental data is reached using the broken symmetry (BS) approach, developed by Noodleman and Norman.[22,23] Application of the BS formalism requires the knowledge of the energies of $2^N/2$ single Slater determinants (where N is the number of exchange coupling constants, J), and this task can easily become difficult for large N.[24] The number of computed determinants was six for both isolated and grafted systems. The BS determinants with different multiplicity were computed on the optimized HS geometries both for the isolated and grafted scenario with a convergence criteria of 1.0×10^{-7} for the wave function energy gradient. We chose to optimize the structures for the high spin (HS, $S = 12$) state in order to avoid problems deriving from an optimization performed on a multideterminant state. The best results for the isolated structures were obtained with the B97 functional with errors below the 3% on the most important distances and angles for both systems in their isolated form (see Figure S1, Supporting Information). The functional B97 was therefore used throughout. Dihedral angles $\alpha_{Mn-N-O-Mn}$, with errors ranging from 1.0 to 10.0 deg, are reported in Table 1.

Table 1. Experimental and Computed Dihedral Angles $\alpha_{Mn-O-N-Mn}$ for Complexes 1 and 2.

complex	data source	$\alpha_{Mn-O-N-Mn}$, deg
1	X-ray[25]	8.9, 25.6, −2.5
		−8.9, −25.6, 2.5
	isolated structure	8.0, 15.0, −9.1
		0.0, −22.9, 9.2
	adsorbed structure	4.1, 13.1, 12.7
		−2.6, −20.3, 16.2
2	X-ray[26]	39.1, 34.9, 43.1
		−39.1, −34.9, −43.1[a]
	isolated structure	37.4, 30.5, 44.8
		−40.7, −32.2, −42.6
	adsorbed structure	39.7, 29.7, 46.0
		−36.4, −32.9, −44.2[a]

[a]Values referred to the [Mn_3] unit closer to the surface.

RESULTS AND DISCUSSION

From the accuracy shown by CP2K in reproducing structural crystallographic data even for such large and complex systems containing several transition metals, we feel confident on the geometrical description of grafting process for **1** and **2**. In ref 13, it was suggested that the local coordination of Mn undergoes an O_h-like rearrangement after grafting. What we have seen is an overall resultant contraction of equatorial Mn−O and Mn−N distances with a concurrent sort of shift for the axial Mn−O distances for both Mn3 units and systems due to the surface compression. The last effect can be directly ascribed to the interaction with the Au(111) surface. On the other hand, Au(111) surface seems to be "plastically" printed by the systems steric shape inducing a depression of about 0.4 Å of the total height of the slab at the deepest point. The optimized structures for the grafted species are reported in Figure 2. The Au(111) surface, as shown in Figure 2, adapts itself to the cluster reflecting its noninnocent effect on the induced distortions on the bottom Mn_3 units in both **1** and **2** . The grafting, in fact, induces an elongation of all Mn−Mn distances from 0.01 to 0.03 Å in Mn_3 units. Larger elongations have been found for Mn−Mn distances connecting the two Mn_3 units for system **2**, probably due to a major steric hindrance of the ligands (see Figure S2, Supporting Information). For system **1**, where interactions $Mn_3\cdots Mn_4$ and $Mn_1\cdots Mn_6$ are propagated via H-bonding and thus are expected to be weak, the following

dx.doi.org/10.1021/jp4009916 | J. Phys. Chem. C 2013, 117, 7186−7190

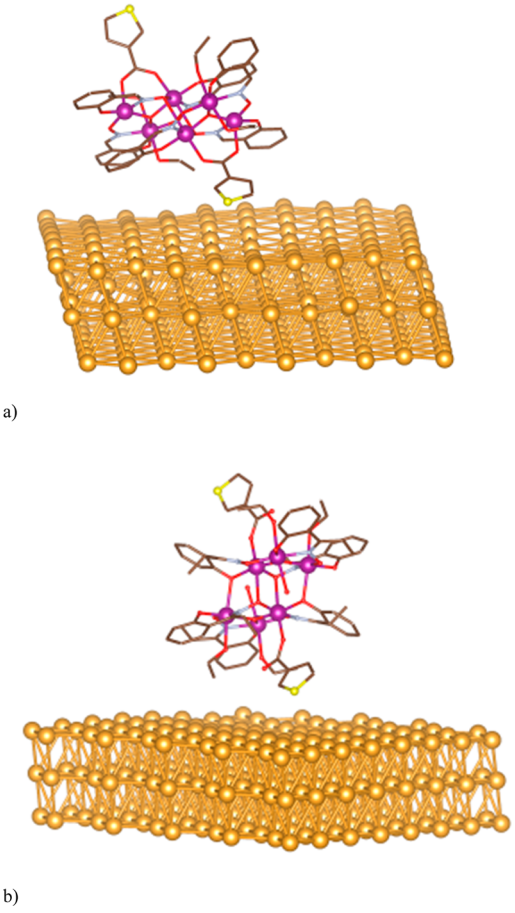

Figure 2. Two $\{Mn_6\}$, **1** (a) and **2** (b), structures grafted on Au(111).[14] Notice the depression induced by the cluster on the gold surface found in (a).

Hamiltonian based on the experimental and computed Mn−Mn distances has been adopted for the isolated and grafted systems

$$SH = J_1(S_1S_3 + S_4S_6) + J_2(S_2S_3 + S_5S_6) + J_3(S_4S_5 + S_1S_2) + J_4(S_1S_4) \quad (1)$$

where the labeling of the paramagnetic centers used is reported in Scheme 1.

Scheme 1. Numbering Scheme Used for Mn Atoms both for Compound 1 and 2.[14]

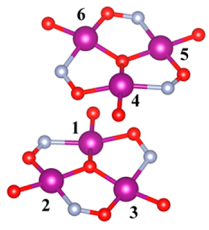

The computed J's are $J_1 = 10.2$ cm^{-1}, $J_2 = 1.6$ cm^{-1}, $J_3 = 3.3$ cm^{-1}, and $J_4 = -2.9$ cm^{-1}. In agreement with the available experimental findings[12] (see also Supporting Information), the computed set of J's leads to an $S = 4$ ground state. A fair agreement is also found with the set of values computed with hybrid functionals reported earlier.[27,28] Antiferromagnetic interactions within the Mn_3 units and ferromagnetic between the Mn_3 units have been reproduced. Moreover, our study confirms the antiferromagnetic coupling for $\alpha < 30°$ (see Table 1 and refs 27 and 28).

Passing to the grafted scenario we have obtained $J_1 = -25.5$ cm^{-1}, $J_2 = 12.9$ cm^{-1}, $J_3 = -5.7$ cm^{-1}, $J_4 = -22.3$ cm^{-1}. Although the ground state S value was not experimentally determined, it was noted that the magnetic properties are likely to be conserved in Au(111).[12,13] Our calculations prove this hypothesis as computed Js on an energy minimized structure yield again an $S = 4$ ground state. Despite the reproduction of the ground state S value, the magnitude and sign of individual exchange are drastically different from those computed for the isolated $\{Mn_6\}$ cluster. Such a result reveals that the gold surface is noninnocent and induces significantly structural modifications. (see Figure S2a, Supporting Information) This is similar to our findings on nitronyl−nitroxides adsorbed on a gold surface.[15]

For complex **2**, (see Scheme 1), we have used the following SH:

$$SH = J_1(S_1S_2 + S_2S_3 + S_1S_3) + J_2(S_4S_6 + S_4S_5 + S_5S_6) + J_3(S_3S_4 + S_1S_6) + J_4(S_1S_4) \quad (2)$$

which reproduces the spin symmetry more properly than the single J SH reported in ref 26. This is also supported by energy degeneracies found for different determinants. The results, using the Scheme 1 labeling, are the following: $J_1 = -37.2$ cm^{-1}, $J_2 = -45.6$ cm^{-1}, $J_3 = -18.81$ cm^{-1}, and $J_4 = -15.5$ cm^{-1}. Passing to the grafted scenario, we obtained the following results: $J_1 = -37.9$ cm^{-1}, $J_2 = -56.4$ cm^{-1}, $J_3 = -36.8$ cm^{-1}, and $J_4 = -21.8$ cm^{-1}. In agreement with the experimental results, we found a $S = 12$ ground state for both isolated and grafted systems. Moreover, ferromagnetic coupling is obtained for $\alpha > 30°$, as predicted (see Table 1 and refs 26−28). Differently from what observed for **1**, where J values changed significantly, for **2** we have confirmed the signs for all J's with an increase of magnitude for all of them but J_1. The larger and more effective differences found for **1** can be justified in terms of different coordination environments. The coordination environment for **1** seems to be less rigid than in **2** and therefore more prone to geometrical rearrangements once grafted on Au(111) surface, as evidenced in Figure S2, Supporting Information. In order to verify if and how the adsorption process could influence the SMM behavior, we have also checked structural and spin parameters. One of them is the average apical-in-plane distance ratio, crucial for the anisotropy parameter of Jahn−Teller distorted Mn(III). Experimentally, values of 1.18 and 1.17 have been reported for **1** and **2**, respectively. Values of 1.207 and 1.176 for the isolated and 1.189 and 1.172 for the adsorbed species have been computed for **1** and **2**, respectively (see Table 2).

The error on the isolated species is less than 3%. These numbers evidence a trend toward a more isotropic environment for Mn(III) passing from the isolated to the grafted scenario for both species. In particular, for **1** the decrease is associated to five of the six Mn ions, with the sixth left unchanged. The largest decrease has been observed for the Mn_3 unit closer to the gold surface. For **2**, instead, the situation is the result of an averaging of opposite distortions between the two Mn_3 units. Actually, the Mn_3 unit interfaced to the gold surface experiences a ratio decrease from 1.177 to 1.162 while the

dx.doi.org/10.1021/jp4009916 | J. Phys. Chem. C 2013, 117, 7186−7190

Table 2. Apical-in-Plane Average Distances Ratio, d_{ax}/d_{eq}, for Optimized Complexes 1 and 2

		Mn(1)	Mn(2)	Mn(3)	Mn(4)	Mn(5)	Mn(6)
1	isolated	1.267	1.122	1.250	1.245	1.101	1.259
	grafted	1.253	1.090	1.233	1.247[a]	1.080[a]	1.233[a]
2	isolated	1.147	1.183	1.196	1.190	1.149	1.192
	grafted	1.186	1.188	1.170	1.178[a]	1.110[a]	1.199[a]

[a]Values referred to the Mn_3 unit closer to the surface.

top Mn_3 unit experiences a smaller ratio increase from 1.175 to 1.181.

Associated to the reduction of the anisotropy in the Mn(III) ion ligand field, we have also computed an overall decrease of the magnetic moments on Mn(III) passing from the isolated to the grafted scenario. For **2**, we have computed the largest decrease (1.4%) while for **1** a decrease of 0.7% is calculated. Such results, even if small in their magnitudes, support the proposed rationalization of XAS and XMCD spectra reported in ref 13. At the geometrical level it is also important to note that the clusters are calculated to be grafted to the surface with the easy axis of the magnetization tilted by an angle of 30° and 15° respect to the normal to the surface for **1** and **2**, respectively. On the basis of such results, we have computed a height of 14.0 and 14.6 Å for cluster **1** and **2** to be compared with an estimate obtained from the crystal structure (16.0 Å) for a standing configuration. This reduction well compares with the value of 11.0 ± 2.0 Å found by the experimental STM line profile for both clusters.[12]

CONCLUSIONS

In conclusion, we have shown that the chosen DF methodology offers reliable spin state structures for SMM grafted on the Au(111). Our results confirm the structural and magnetic robustness of $\{Mn_6\}$ clusters previously evidenced by synchrotron-based investigations. The computational approach presented here seems therefore to represent a precious tool to pick out molecular structures that are more likely to retain their SMM character once are grafted to a conducting substrate, thus allowing to focus experiments on the most promising systems.

ASSOCIATED CONTENT

Supporting Information

Additional information on computation of J values using a different spin Hamiltonian along with an overlay of optimized geometries in comparison to the X-ray structure and an overlay plot of $\{Mn_6\}$ structure in SAM and isolated scenario are given. This material is available free of charge via the Internet at http://pubs.acs.org.

AUTHOR INFORMATION

Corresponding Author

* E-mail: (F.T.) federico.totti@unifi.it.

Notes

The authors declare no competing financial interest.

ACKNOWLEDGMENTS

We acknowledge the CINECA award under the ISCRA initiative, for the availability of high performance computing resources and support. The support of the ERC through the AdG MolNanoMaS (Project No. 267746) and of the Italian MIUR through the FIRB project "Nanomagneti molecolari su superfici metalliche e magnetiche per applicazioni nella spintronica molecolare" (RBAP117RWN) are also acknowledged. G.R. would like to acknowledge the financial support from the Government of India through Department of Science and Technology (SR/S1/IC-41/2010 and SR/NM/NS-1119/2011).

REFERENCES

(1) Cornia, A.; Fabretti, C.; Zobbi, L.; Caneschi, A.; Gatteschi, D.; Mannini, M.; Sessoli, R. In *Single-molecule magnets and related phenomena*; Winpenny, R., Ed.; Structure and Bonding 122; Springer: Berlin and Heidelberg, Germany, 2006; p 133.
(2) Bogani, L.; Wernsdorfer, W. *Nat. Mater.* **2008**, *7*, 179.
(3) Gatteschi, D.; Sessoli, R.; Villain, J. *Molecular Nanomagnets*; Oxford University Press: Oxford, U.K., 2006.
(4) Lin, P.-H.; Burchell, T. J.; Ungur, L.; Chibotaru, L. F.; Wernsdorfer, W.; Murugesu, M. *Angew. Chem., Int. Ed.* **2009**, *48*, 9489.
(5) Blagg, R. J.; Muryn, C. A.; McInnes, E. J. L.; Tuna, F.; Winpenny, R. E. P. *Angew. Chem., Int. Ed.* **2011**, *50*, 6530.
(6) Ishikawa, N.; Sugita, M.; Ishikawa, T.; Koshihara, S.-Y.; Kaizu, Y. *J. Am. Chem. Soc.* **2003**, *125*, 8694.
(7) Rinehart, J. D.; Fang, M.; Evans, W. J.; Long, J. R. *Nat. Chem.* **2011**, *3*, 538.
(8) T. Rajeshkumar, T.; Rajaraman, G. *Chem. Commun.* **2012**, *48*, 7856.
(9) Milios, C. J.; Vinslava, A.; Wernsdorfer, W.; Moggach, S.; Parsons, S.; Perlepes, S. P.; Christou, G.; Brechin, E. K. *J. Am. Chem. Soc.* **2007**, *129*, 2754.
(10) Grumbach, N.; Barla, A.; Joly, L.; Donnio, B.; Rogez, G.; Terazzi, E.; Kappler, J.-P.; Gallani, J.-L. *Eur. J. Phys. B* **2010**, *103*, 73.
(11) Mannini, M.; Pineider, F.; Danieli, C.; Totti, F.; Sorace, L.; Sainctavit, Ph.; Arrio, M.-A.; Otero, E.; Joly, L.; Cezar, J. C.; Cornia, A.; Sessoli, R. *Nature* **2010**, *468*, 417.
(12) Moro, F.; Corradini, V.; Evangelisti, M.; De Renzi, V.; Biagi, R.; del Pennino, U.; Milios, C. J.; Jones, L. F.; Brechin, E. K. *J. Phys. Chem. B* **2008**, *112*, 9729.
(13) Moro, F.; Corradini, V.; Evangelisti, M.; Biagi, R.; De Renzi, V.; del Pennino, U.; Cezar, J. C.; Inglis, R.; Milios, C. J.; Brechin, E. K. *Nanosacale* **2010**, *2*, 2698.
(14) Momma, K.; Izumi, F. VESTA 3 for three-dimensional visualization of crystal, volumetric and morphology data. *J. Appl. Crystallogr.* **2011**, *44*, 1272.
(15) Rajaraman, G.; Caneschi, A.; Gatteschi, D.; Totti, F. *J. Mater. Chem.* **2010**, *20*, 10747.
(16) Rajaraman, G.; Caneschi, A.; Gatteschi, D.; Totti, F. *Phys. Chem. Chem. Phys.* **2011**, *13*, 3886.
(17) Mundy, C. J.; Mohamed, F.; Schiffman, F.; Tabacchi, G.; Forbert, H.; Kuo, W.; Hutter, J.; Krack, M.; Iannuzzi, M.; McGrath, M.; Guidon, M.; Kuehne, T. D.; Laino, T.; VandeVondele, J.; Weber, V. CP2K software package, http://cp2k.berlios.de.
(18) Tao, J.; Perdew, J. P.; Staroverov, V. N.; Scuseria, G. E. *Phys. Rev. Lett.* **2003**, *91*, 146401.
(19) Zhang, Y.; Yang, W. *Phys. Rev. Lett.* **1998**, *80*, 890.
(20) Becke, A. D. *J. Chem. Phys.* **1997**, *107*, 8554.
(21) Grimme, J. *J. Comput. Chem.* **2006**, *27*, 1787.
(22) Noodleman, L.; Norman, J. G., Jr. *J. Chem. Phys.* **1979**, *70*, 4903.
(23) Noodleman, L. *J. Chem. Phys.* **1981**, *74*, 5737.
(24) Bencini, A.; Totti, F. *J. Chem. Theory Comput.* **2009**, *5*, 144 and references therein..

(25) Milios, C.; Raptopoulou, C. P.; Terzis, A.; Lloret, F.; Vicente, R.; Perlepes, S.; Escuer, A. *Angew. Chem., Int. Ed.* **2004**, *43*, 210.
(26) Milios, C. J.; Inglis, R.; Vinslava, A.; Bagai, R.; Wernsdorfer, W.; Parsons, S.; Perlepes, S. P.; Christou, G.; Brechin, E. K. *J. Am. Chem. Soc.* **2007**, *129*, 12505.
(27) Atanasov, M.; Delley, B.; Neese, F.; Tregenna-Piggott, P. L.; Sigrist, M. *Inorg. Chem.* **2011**, *50*, 2112.
(28) Cremades, E.; Cano, J.; Ruiz, E.; Rajaraman, G.; Milios, C. J.; Brechin, E. K. *Inorg. Chem.* **2009**, *48*, 8012.